

Markovian Memory Embedded in Two-State Natural Processes

Fotini Pallikari

*University of Athens, Faculty of Physics, Department of Solid State Physics,
Panepistimiopolis Zografou, 15784 Athens, Greece**

Nikitas Papasimakis

Optoelectronics Research Centre, University of Southampton, Southampton SO17 1BJ, United Kingdom

Markovian type of memory is considered as an inseparable ingredient in a variety of natural two-state processes within a vast range of interdisciplinary fields. When binary processes are considered, the Markovian memory embedded in their natural evolution introduces either clustering or dispersion of binary states. Markovian memory can even imitate the evolution of a random process, regarding the long-term behavior of the frequencies of its binary states. This occurs when the associated binary self-transition state probabilities are balanced. In the present work Markovian memory is introduced into three processes originating from diverse fields, such as handedness in nonhuman troglodytes, the Quantum Zeno effect and the formation of two-dimensional magnetic domains. The aim being to illustrate the merits, the wide range applicability of the approach and the variety of information it provides as regards the dynamics of the process.

INTRODUCTION

Markov sources provide phenomenological representations of a wide range of natural processes. In a Markov chain involving state measurements, the system under observation experiences state transitions according to specified probabilities. A specific class of Markov sources are the two-state systems, frequently employed in physics on a multitude of occasions such as to represent spins in the Ising model, or the outcome of particle collisions in the Galton board binomial experiment[1]. Binary systems can also represent sequences of quantum measurements, as in the case of the quantum Zeno effect(QZE), where the natural evolution of the two-level atomic system is hindered by rapid observations [2, 3]. Moreover, binary systems are often encountered in electronic solid-state diffusion [4], turbulent flow dynamics [5, 6, 7], bistable liquid crystal displays [8, 9, 10], Josephson junctions [11], or flip-flop electrical circuits in computing machines, which fit well as types of two-state systems [12]. Binary Markov processes can, therefore, describe adequately a whole host of physical micro- as well as macro-systems [13].

Yet, two state systems are not only pertinent in physics and computing, but also highly relevant to probabilistic systems commonly studied within the medical and social sciences. It is customary, for instance, in medicine [14], psychiatry [15], or anthropology [16], to test a hypothesis against two alternatives. In medicine, the effect of a drug treatment is decided from the proportion of successes (against failures) across many independent studies. While the degree of reliability of the results depends on the trustworthiness of the database, specific tests are designed to determine whether the database is free from biases. One such mainly visual test is the construction of a scatter plot of independent results that constitute the database [17]. If the distribution of a large number of data on the scatter plot appears asymmetric, it implies that the database is biased by, as an example, publication biases and thus rendered inappropriate source for reliable statistical inferences regarding the studied effect. Less emphasis has been sited so far on the scatter plot's breadth and the information that it can provide concerning the dynamics of the underlying mechanism. The relationship between them, however, can be exemplified on the basis of two-state Markov processes, as will be shown in this work.

Markovian memory is introduced by the requirement that each new state depends on previous states some n steps back, so that past probabilities determine the future ones [18, 19]. As it is discussed here, the dynamics of two-state systems fall under two specific categories of Markovian memory, which either introduce a clustering or a dispersion of binary states.

A brief description of the two-state Markov process is offered in section 2. The statistics of Markov chains in relation to the clustering and dispersion of states is discussed in section 3. Three applications of the mathematical approach implicating Markovian memory, in physics (QZE & Ising model) and anthropology (Handedness) are presented in section 4. A more detailed analysis of the present mathematical treatment is provided in the appendix.

FIRST-ORDER, TWO-STATE MARKOV PROCESS

A first-order, two-state Markov process is driven by four transition probabilities, p_{ij} , $i, j = 1, 2$. The sequence of measurements of the binary state, x_n , represents the occurrence of an event (state A), otherwise exemplified by $x_n = 1$, or the failure of its occurrence (state B) corresponding to $x_n = 0$. The initial absolute probabilities of finding the system at either state A or B are p_1 & $1 - p_1$, respectively. Once the system is at state A, the conditional probability that it remains at the same state after a single measurement is $p_{11} = p$, whereas the conditional probability, p_{21} to make a transition to B will be $1 - p$. In a similar fashion, probabilities $p_{22} = q$ and $p_{12} = 1 - q$ are assigned to transitions from state B. In both cases, the self-transition probabilities satisfy the inequality $0 < p, q < 1$. Whereas $p, q = 0.5$ underlines random variability of state measurements, the range of probabilities $0.5 < p, q < 1$ and $0 < p, q < 0.5$ introduce persistence of the same state and anti-persistence, respectively, while the latter case implies an increased probability to avoid transitions to the same state over a sequence of measurements. We shall next discuss how the expected frequency of the one state of the Markov process (A), in a sequence of n consecutive measurements, depends on the self-transition probabilities p & q .

The average frequency, \bar{p}_n , of occurrence of state A in a Markov chain of n steps is [20]

$$\bar{p}_n = \wp + \frac{p_1 - \wp}{n} \cdot \frac{1 - a^n}{1 - a} \quad (1)$$

The parameter $a \neq 1$ is

$$a = p + q - 1 \quad (2)$$

After a large enough number of state measurements, n , (Markov transitions) the frequencies of observed states A and B become \wp and $1 - \wp$, respectively, at any value of parameter a .

$$\wp = \lim_{n \rightarrow \infty} p_n = \frac{1 - q}{2 - (p + q)}$$

$$1 - \wp = \frac{1 - p}{2 - (p + q)} \quad (3)$$

If $p = q \neq 0.5$ then $\wp = 0.5$. This curious result turns a Markov process with memory into a random process, as far as the long-term state frequency \wp , is concerned.

Yet, the non-randomness of the Markov process is directly observed through the variance of the binary state in the sequences. The standard deviation of the expected proportion of binary state A, \bar{p}_n , is estimated to be [20]

$$\sigma = \sqrt{\frac{\wp(1 - \wp)}{n}} \cdot \sqrt{\frac{p + q}{2 - (p + q)}} \quad (4)$$

Relation (4) is also written $\sigma = \sigma_0 \cdot \nu$, where $\sigma_0 = \sqrt{\wp(1 - \wp)/n}$, is the standard deviation of outcomes of a memory-free Markov process and it indicates that the variance of \bar{p}_n can be modulated by a factor $\nu^2 \neq 1$ introduced by the Markov self-transition probabilities p & q . Assuming $p \& q \neq 0.5$ the factor which modulates the variance is

$$\nu^2 = \frac{p + q}{2 - (p + q)} \quad (5)$$

A large variety of natural processes can be represented as Markov processes. In such cases the characteristic parameters \wp and ν^2 can be assigned accordingly. These provide insights in the process dynamics on first neighbor level. Often a process is studied through its statistical behavior with the help of meta-analyses. In such approaches, the two characteristic parameters, \wp & ν^2 , can be easily estimated through the so-called scatter plots. The application of the Markov process on such statistical ensembles can provide useful information on the investigated process as will be shown next.

SCATTER PLOT OF MARKOVIAN BINARY STATES

The combination of results from independent studies of a phenomenon constitutes the so-called meta-analysis. The accuracy of the result of each individual study depends proportionally on the size, n , of the study, since the associated error is inversely proportional to the square root of the standard deviation.

The scatter plot, $n = f(\bar{p}_n)$, where the size of studies, n , is plotted against the associated proportion of binary state, \bar{p}_n , will be shaped like an inverted funnel [21] centered at \wp , the single true average, or in other words the value to which the averages \bar{p}_n converge. This is due to the fact, as mentioned above, that the estimate of the underlying effect becomes more accurate as the sample size of component studies increases. Scatter plots can thus provide useful information not only on the magnitude, \wp , of an investigated effect, but also about the dynamics of the mechanism involved [22].

The frequency of state A, \bar{p}_n , in a sequence of n individual measurements of a Markov process will range within a confidence interval. The 95% of them are expected to be enclosed in the scatter plot by the confidence interval, represented by the two funnel-shaped red curves in Fig. 1, $\bar{p}_n = f(n)$ or $n = f(\bar{p}_n)$

$$\bar{p}_n = \wp \pm 1.96 \cdot \sqrt{\frac{\wp(1-\wp)}{n}} \cdot \nu \quad (6)$$

and

$$n = 3.84 \cdot \frac{\wp(1-\wp) \cdot \nu^2}{(\bar{p}_n - \wp)^2} \quad (7)$$

Computer-simulated Markovian data sequences of size n were generated and plotted against the frequency of binary state A, p_n , in each sequence. Fig. 1 illustrates two such examples; (a) one of a symmetric ($p = q$) Markov process exhibiting anti-persistence, $p, q < 0.5$, and (b) of an asymmetric ($p \neq q$) Markovian process with $p = 0.88$, $q = 0.5$ exhibiting one-sided persistence. In the symmetrical case, $p = q$, the correlation factor C_m between the two states in the Markov chain

$$C_m = \lim_{N \rightarrow \infty} \frac{1}{N} \sum_{n=1}^N s_n s_{n+m} \quad (8)$$

becomes the assemble expectation value of the correlation between first-order neighbors [23]

$$C_1 = \langle s_n s_{n+1} \rangle = 2p - 1 \quad (9)$$

When $p = q = 0.88$ the strong, positive correlation of neighbors ($C_1 = +76\%$) introduces persistence and therefore clustering of states, while the condition $p = q = 0.12$ introduces strong negative correlation, anti-persistence and dispersion of states ($C_1 = -76\%$). The graphical representation of Fig. 1 confirms that the simulated Markovian data obey well the statistical estimations: the 95% of them were found enclosed under the two 95% confidence interval curves, Eq. (7), suggesting that this statistical tool applied on scatter plots of meta-analyses is relatively reliable.

The modulated variance, as described above, indicates absence of random variability in independent measurements of an effect [24]. This type of observed irregularity within a meta-analysis has been referred to by the term "statistical heterogeneity" [25]. There are numerous reasons possible behind statistical heterogeneity in a database. We consider here the two types that generate either dispersion or clustering of Markovian states.

Looking closer at the shape of the plot we notice that, according to Eqs. (4) & (5), when $\nu > 1$ its scatter becomes broader at all N , as compared that of a memory-free process ($\nu = 1$). Similarly, the variance will be narrowed in the case where $p + q < 1$, (i.e. $\nu < 1$). The broadening of a scatter plot is the direct consequence of the persistence of a binary state and the occurrence of longer-than-usual runs in the data sequences due to state clustering, as Fig. 2 clearly illustrates.

It is expected that, when $p = q = 0.5$, the number of runs having length m , a_m , i.e. sequences of the same binary state occurring at frequency \bar{p}_n in a sequence of total length n , will be [20]

$$a_m = (n - m - 1) \cdot [\bar{p}_n^2 (1 - \bar{p}_n)^m + (1 - \bar{p}_n)^2 \bar{p}_n^m] \quad (10)$$

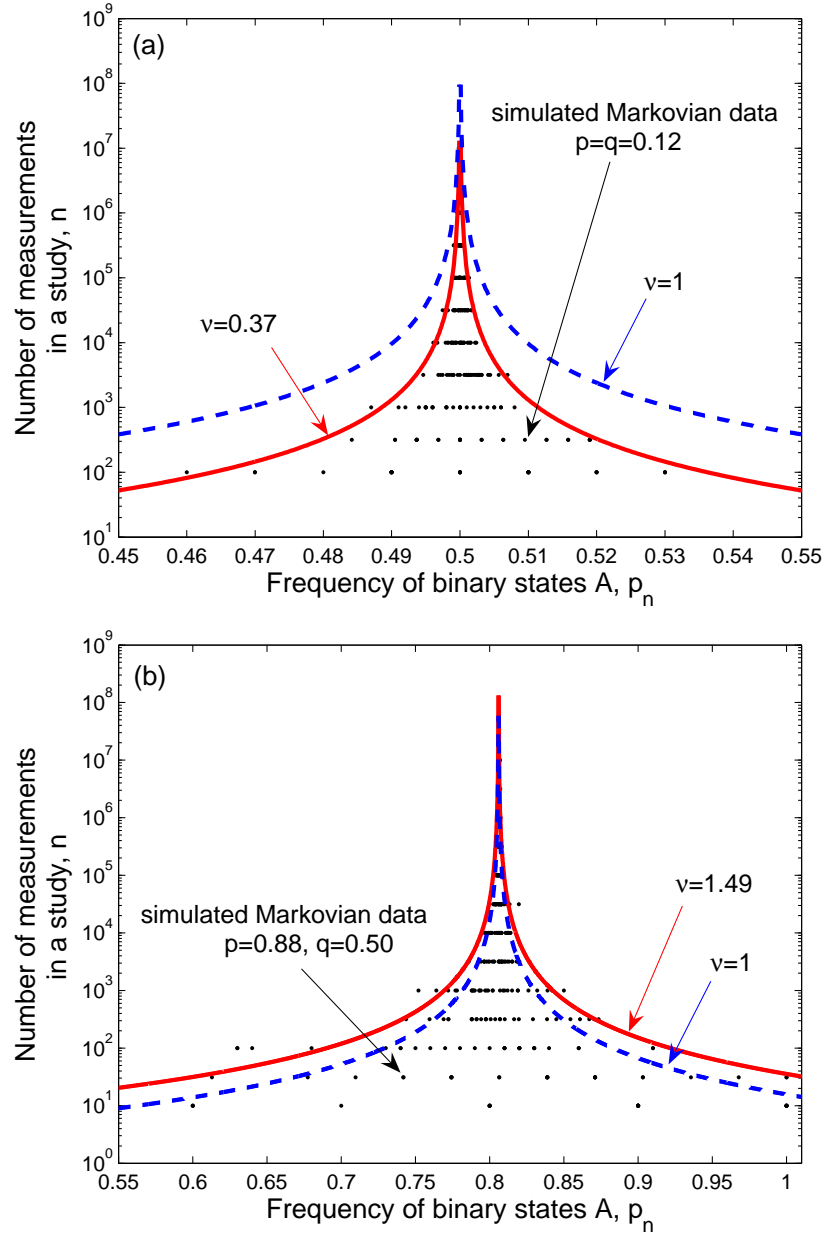


FIG. 1: Scatter plot of Markovian data. Squares: computer simulated data.: (a) Solid lines: Symmetric Markovian process, $p = q = 0.12$, $\nu = 0.37$ & $\varphi = 0.5$. Probabilities $p, q, < 0.5$ introduce anti-persistence and $\nu < 1$ introduces dispersion of states & narrowing of variance. Dotted lines: memory-free binary process, $\nu = 1$. (b) Solid lines: Asymmetric Markovian process, $p = 0.88$ & $q = 0.5$, $\nu = 1.49$, $\varphi = 0.81$. The persistence introduced by the self-transition probability, p , of state-A, introduces broadening of the variance ($\nu > 1$), according to relation (4) and as compared to a Markov process with $\varphi = 0.81$ & $\nu = 1$.

The variance σ of a_m for long enough sequences is: $\sigma = a_m$. In Fig. 2 the normalized average number of runs (over 10 computer-simulated symmetric Markov sequences, each of length $n = 10,000$), is plotted against the length of run, m . When the Markovian memory ($p = q = 0.88$) introduces persistence and clustering of the same binary state, the average length of the computer-simulated runs is considerably longer than that of the memory-free case ($p = q = 0.5$). On the contrary, in the anti-persistent case ($p = q = 0.12$), the average length of runs is shorter than that of the memory-free sequences. This result supports that, in the latter condition, the states tend to disperse. The simulated Markovian memory-free sequences, on the other hand, behave according to Eq. (9), as expected [26] by

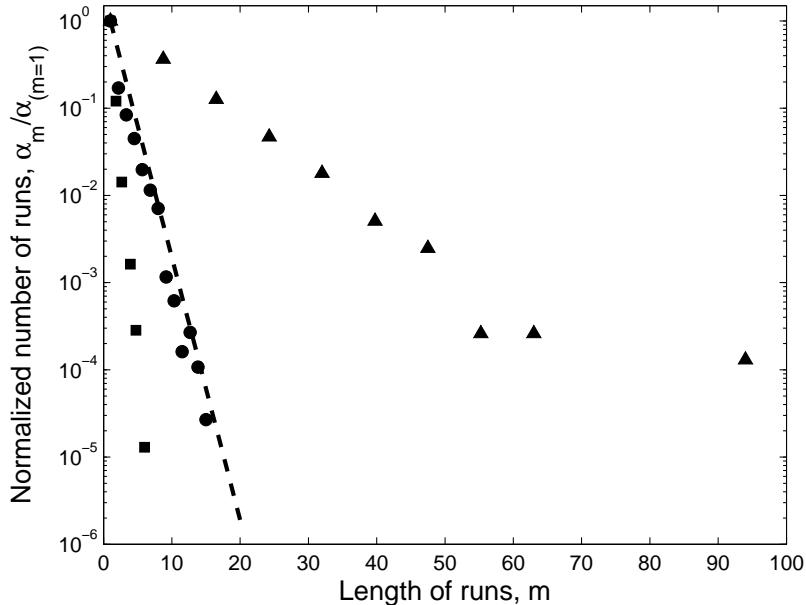


FIG. 2: Normalized length of run (averaged over 10 sequences) in a 10,000-unit long computer generated Markovian sequence. (a) *Circles*, $p = q = 0.50$, memory-free Markovian process; (b) *triangles*, $p = q = 0.88$, clustering of states; (c) *squares*, $p = q = 0.12$, dispersion of states; (d) *dotted line*: theoretical expectation for memory-free processes, Eq. (10).

theory. Estimating the self-transition probabilities (p, q) and the variance factor ν^2 provides a quantifiable description of the Markovian dynamics in natural processes within a diversity of scientific disciplines.

We have selected three exemplars to illustrate the extent of applicability of the current Markovian analysis. The first one investigates the correlations within anthropological observations in handedness. In the second example the analysis is applied to the Markovian characteristics of the quantum Zeno effect. Finally, in the third example, we investigate the formation of magnetic domains in solid state as a Markovian process.

EXAMPLES OF THE MARKOV MEMORY MODEL IN NATURAL PROCESSES

Handedness as a Markov process

Often in scientific disciplines such as medicine, anthropology, sociology, or psychology the evaluation of evidence regarding an effect makes use of scatter plots. On one such occasion within anthropology, a meta-analysis, that merged the results of 32 studies, was performed to investigate the strength and consistency of right-handedness in nonhuman primates [16], Fig. 3. This application refers to an even blend of primates raised in the wild as well as in captivity. The constructed scatter plot in this study was intended to shed light on questions regarding the consistency of the data variability with normal sampling variation and the nature of biases in the reports of statistically significant handedness. One could, however, get additional information from these scatter plots, with regard to the internal dynamics of the processes involved that lead to handedness preference.

We assume that the interactions among the nonhuman primates which influence handedness are driven by a Markovian binary process, where preference for the right and left hand is represented by the self-transition probabilities, p & q , respectively. The scatter plot of Fig. 3 graphically outlines the confidence interval curves of Eq. (7) that best envelope the 95% of these data. In the present example, the number, n , of right-handed individuals (pan troglodytes) among those found to be significantly handed was plotted against the study's effect size (frequency) \bar{p}_n . The confidence interval curves that best envelope the 95% of data points shown in Fig. 3, are given by

$$n = \frac{1.24}{(\bar{p}_n - 0.58)^2} \quad (11)$$

These involve the Markovian parameters: $p = 0.64$ & $q = 0.50$, $\nu = 1.15$ and $\varphi = 58\%$. The confidence interval representing random variability data ($\nu = 1$), which implies an equal preference for right and left hand use, is also marked on the graph for comparison, and it is clearly not fitting adequately the totality of these data. The accuracy of the three parameters above is limited to 1% and so the parameters are rounded up to the second decimal digit [27]. It is a known fact that handedness among the members of a group tends to be positively correlated, so that the estimated self-transition probabilities for either the use of the right or the left hand could be > 0.5 . The combination of this hypothesis with the condition that the 95% of the data points should be enveloped by the confidence interval curves enables a relatively accurate adjustment of the two parameters, p & q , hindered only by the limitations of the size of this database.

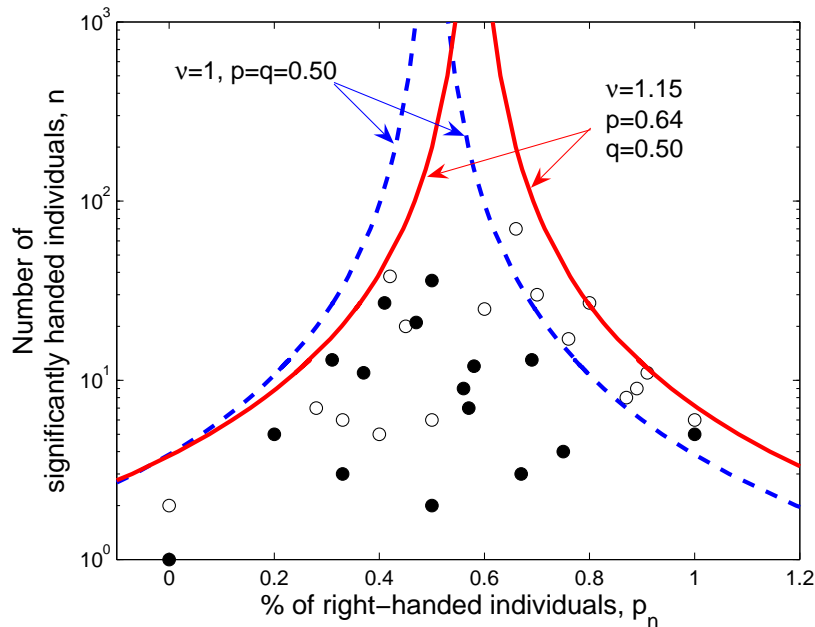


FIG. 3: Scatter plot of a meta-analysis investigating preference in handedness among nonhuman primates [16]. Open circles: captive, closed circles: individuals in the wild. The 95% confidence interval curves are also plotted (solid curves), Eq. (7), suggesting that $\varphi = 0.58$, $p = 0.64$ & $q = 0.50$, $\nu = 1.15$. Dotted lines: memory-free & symmetric Markov process ($\varphi = 0.5$, $\nu = 1$). See text for details.

The estimated parameters imply that 58% of the individuals are right-handed. It comes as the consequence of a 64% probability that individuals influence each other to use the right-hand, at variance with a mere 50% probability for the use of the left hand. The scatter plot further indicates that among the studied population the bilateral individuals are generally those raised in the wild (dark circles). Also, that the average being above 50% is mainly due to the contribution from individuals in captivity (open circles). If only chimps in the wild are considered in the scatter plot, the estimated parameters become $p = q = 0.5$ $\varphi = 0.5$ and $\nu = 1$ indicating true bilateral handedness.

These results harmonize with findings from anthropological studies. Anthropologists discovered that chimpanzees develop cultures in the same way as humans do. According to Whiten et al. [28], handedness in nonhuman primates tends to be lateralized. Yet, unlike humans where there is only 10% use of left hand, this proportion in nonhuman primates in the wild reaches 50%. Chimps in captivity, however, exhibit a weak preference for the use of right hand, which is believed to result from the human influence. This is exactly inferred from the Markov memory analysis.

The quantum Zeno effect

The second application of the Markov memory model relates to quantum theory. More specifically, it involves the prediction [2] and the experimental observation [3] of the quantum Zeno effect (QZE), where the transitions of a bistable quantum system are impeded by repetitive state measurements. On the other hand, a hindering of the binary state will introduce persistence of state in a series of measurements and cause the generation of longer runs of the

same state. The QZE systems represent, therefore, attractive candidates for the application of the Markov memory analysis from which the associated self transition probabilities can be deduced.

In this example, bi-stability in a three-level system operates between the two lower states, 1 and 2. If the system is initially at state 1, it can make transitions to higher energy states 2 and 3, driven by a field of appropriate frequency. Its transition to state 2 is effected by a square pulse of duration T , (*the driving field*), while its transition to state 3 is effected by a series of n pulses of the measurement or probe field, applied equidistantly during the period T . Only stimulated transitions between states 2 and 1 are possible. Spontaneous decay from state 3 to 2 is not allowed. However, the relaxation from state 3 to state 1 is fast and is used to probe the state of the bistable system.

The estimation of the Markovian probabilities shows that in the studied QZE experiment, Balzer et al have observed both clustering as well as dispersion of binary states. More precisely, the experiment refers to the atomic transitions between two states of the ion $^{172}\text{Yb}^+$ driven by 411 nm quasi-monochromatic light. The probe light pulses operate at 369 nm. When the system is found at state-1 (ground state) this is registered as 'on' measurement, while if it is at the state-2 (excited metastable) this is registered as 'off' measurement. Sequences of measurements labeled 'on' or 'off' (runs) were consequently generated. The generation of longer or shorter runs of 'on' and 'off' measurements having statistical nature depends on the applied experimental conditions.

It is known that once the system begins from a given binary state, the probability that it makes a transition to the other state is $(G^2/\Omega_R^2) \cdot \sin^2(\Omega_R/2 \cdot \tau)$ and the probability that it remains at the same state is $1 - (G^2/\Omega_R^2) \cdot \sin^2(\Omega_R/2 \cdot \tau)$, where $\Omega_R = \sqrt{(\omega - \omega_o)^2 + G^2}$ is the Rabi frequency, G is the field-matter interaction factor, τ is the probe pulse duration and $\omega - \omega_o$ is the frequency detuning between the driving light, ω , and the atomic resonance, ω_o . The probability to find the system at the other state would be, therefore, altered either through changing the rate of probe pulses (τ), or through the detuning factor ($\omega - \omega_o$), which was actually the method employed in reference [3]. The clustering of states was observed in the graphical representation $N_m = f(m)$ of the number of sequences of m identical events [29], N_m , normalized by the number of runs of length $m = 1$ against the length of run, m , for three different settings of the frequency detuning $\omega - \omega_o$.

Simulations of runs of Markov sequences were fitted on the experimental QZE data of Balzer et al, in order to estimate the associated Markovian self-transition probabilities, p_{11} & p_{22} as shown in Fig. 4. The three frequency-detuning experimental settings had been chosen to lie close to the principal resonance ω_o . In the first experimental setting (denoted as setting #7), the system starts from the excited state 2 at conditions favoring persistence of this state (i.e. minimum transition probability). The Markov model fitted to these data estimated the self-transition probabilities to be $p_{22} = 0.65$ and $p_{11} = 0.25$. The chosen experimental conditions, therefore, have lead to persistence of the 'off' state-2 due to a combination of a 65% preference for this state and additionally and most effectively, a 75% probability of avoiding (anti-persistence) the 'on' state-1. The combined mild preference for state-2 and strong avoidance of state-1 has had the result to impede the state transitions leading to persistence of state-2. Longer runs of state-2 will be generated as Fig. 4 indeed confirms.

The other two settings, 6 & 5, characterize higher and lower degrees of detuning than the one before, respectively. Lower detuning, case #5, introduces a higher probability of transition from the excited 'off' state, so that the ground 'on' state will be favoured. In terms of the applied Markov model, this would make the runs of ground state-1 to become longer, mainly due to the relatively high self-transition probability (80%), which causes a relatively strong persistence of state-1. On the other hand, the Markov self-transition probability of the excited state-2 is close to the memory-free case, 55%, so that persistence of state-1 is mainly driven by its high self-transition probability. Even higher detuning levels will entirely disrupt transitions from the excited state as in case #6, such as to give rise to similar and relatively low levels of persistence in both the ground and excited state. The estimated Markov self-transition probabilities are $p_{11} = 0.60$ and $p_{22} = 0.65$.

This example shows how the QZE can be alternatively be accounted for as a process driven by a Markovian type of memory. The agreement between simulated and experimentally observed QZE data is very good, especially for frequencies up to about 10^{-4} .

Ising model & spin domain patterns

This last example applies the Markov memory process on the formation of magnetic domains in ultra thin films. Iglesias et al [30] performed Monte Carlo simulations to generate two-dimensional magnetic domain patterns, with the use of a classical Ising-like Hamiltonian based on long-range interactions. One Monte Carlo step (MCS) refers here to the successive updating of spins chosen at random, according to the Metropolis procedure. Thus, the simulated domains had created three types of formations depending on the applied potential, namely 'stripes', 'cells' and 'labyrinth'. Of all three formations the largest area is covered by the labyrinth shaped domains. The application

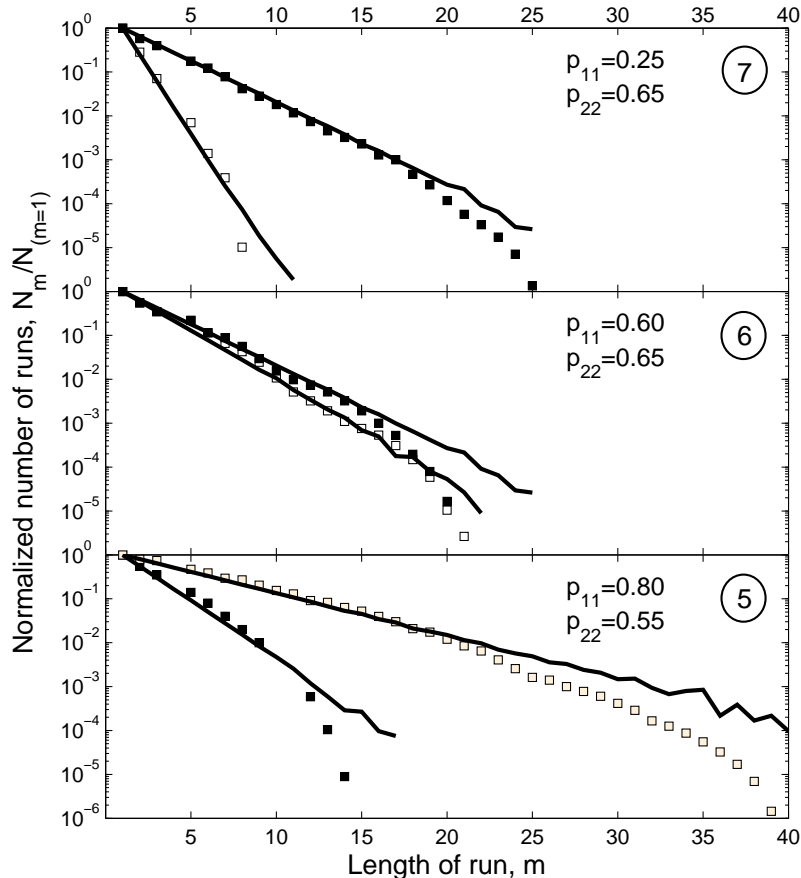


FIG. 4: Clustering and dispersion of Markovian states in the quantum Zeno effect. Experimental data for three different detuning settings indicated as 5, 6, & 7 [3, 31]. Open squares: 'on' events, state 1. Dark squares: 'off' events, state 2. Lines: computer simulated runs of a two-state Markov memory process, modulated by the self-transition probabilities, p_{11} & p_{22} . See text for details.

of the Markov model on the characteristics of the simulated domains allows for the estimation of the prevailing self-transition probabilities between spin states that lead to these three specific formations.

The system is seen to reach a steady-state after the first 30 MCS. The size of stripes and labyrinth configurations are markedly smaller than the average size of cell. To find out what are the Markovian memory self-transition probabilities that have generated such domains, we first convert the size of the 2D domain area into a 1D equivalent as follows. Imaginary straight lines cutting through the 2D magnetic domains would mark along their path stretches (runs) within which the spins are found either up or down. The average length of those stretches, being statistically independent of orientation, is equivalent to the average length m of a run of like-spins. Assuming that the whole 2D simulation is intersected by a square grid, the average size of simulated domain (Fig. 3 of reference 30) will be equivalent to the size of the square whose side is the one-dimensional run length, m .

Since $M \simeq 0$, it makes sense to assume that the generation of 2D magnetic domains has the characteristics of a two-state Markovian procedure driven by equal self-transition probabilities, $p = q$, as will be shown. The case of labyrinth formations at very low temperatures is an exception. If we denote the two spin states by $S_i = \pm 1$, then the magnetization is proportional to the sum of the series S_i

$$M \sim \sum_{i=1}^L S_i \quad (12)$$

TABLE I: Conversion of the size of simulated two-dimensional magnetic domains, from data of Fig. 3 in reference [30], into one-dimensional run lengths for each of stripes, labyrinth and cells formations depending on the applied conditions. The estimated Markovian self-transition probability p , refers to the occurrence of spin state $S_i = +1$.

| Domain Type | 2-D Domains | 1-D Run Length | p |
|------------------|-------------|----------------|-------|
| <i>Stripes</i> | 25.6 | 5.060 | 0.802 |
| <i>Labyrinth</i> | 44 | 6.633 | 0.845 |
| <i>Cells</i> | 150 | 12.247 | 0.918 |

where L is the length of the series. Assigning the probability of each unit $S_i = \pm 1$ in a long sequence of states as \wp and $1 - \wp$, respectively, the magnetization ($-1 < M < 1$) becomes

$$M \sim \wp \cdot (+1) + (1 - \wp) \cdot (-1) \sim 2 \cdot \wp - 1 \quad (13)$$

From Eqs. (13) & (3) we find how the magnetization M (excluding $M = 1$) depends on the self transition probabilities, p & q ,

$$q = \frac{1 + M}{1 - M} \cdot p - \frac{2M}{1 - M} \quad (14)$$

Obviously, $M \simeq 0$ when $p = q$, which is the case for both stripes and labyrinth formations at all temperatures. This result justifies the assumption made earlier that here the self-transition probabilities are taken to be equal.

The magnetization of the cells configuration is -1 at very low temperatures. It rises linearly from -1 to 0 with temperature and becomes zero above the critical temperature. The absolute difference between the two self-transition probabilities, $|p - q|$, then gradually decreases to reach zero when $M = 0$. At such very low temperatures, where $M = -1$, the self-transition probability equals $q = 1$ marking a maximum persistence of the spin state assigned by $S_i = -1$, while the probability of the other state, $S_i = +1$, can take any values within the range $0 \leq p < 1$. Excluding this case, therefore, we can safely assume $p = q$ for a wide range of temperatures.

Markov memory self-transition probabilities were gradually increased from 0.001 to 0.999 by a step of 0.001. The initial probability to observe the state $S_i = +1$ is assumed $p_1 = 0.5$. For every pair of values p, q , 100 Markov chains were simulated each having length $L = 200$, according to the original set up applied by Iglesias et al. The number of runs a_m , with length m , is estimated for each Markov chain. Obviously, the sum of all non-overlapping runs should be equal to the length L : $\sum_m (a_m \cdot m) = 200$. The average length, N , of runs is estimated as

$$N = \frac{\sum_m (a_m \cdot m)}{\sum_m a_m} \quad (15)$$

For self-transition probability p , the average run length of N , $N_{p,q}$, is estimated from the set of 100 generated Markov chains. Finally, the graph $N_{p,q} = f(p, q)$ is plotted and fitted to the estimated by Iglesias et al 1D domain size. The graph when $p = q$, Fig. 5, gives the probability p that a spin state $S_i = +1$ occurs after the same spin state has been registered, Table 1. The state self-transition probabilities assigned to the spin interactions in all three formations are relatively high, above 80% with the highest (92%) occurring in the case of cells, being the largest in size of all other simulated magnetic formations.

Alternatively, the condition $p \neq q$ would imply that the two spin states (up & down) are not equally probable. This asymmetric condition would occur when, for instance an external magnetic field is applied favoring the one of the two spin orientations. It could also occur at very low temperatures when large size magnetic domains are formed as is the case with cells.

SUMMARY

In this work it is shown that Markovian memory embedded in natural processes provides an alternative quantitative as well as qualitative description of a wide interdisciplinary range of processes, classified as two-state systems. Once memory is present within the Markovian process, [32] this will lead to either clustering of binary states and broadening of the variance, observed in a scatter plot of individual studies, or dispersion of states and narrowing of the scatter

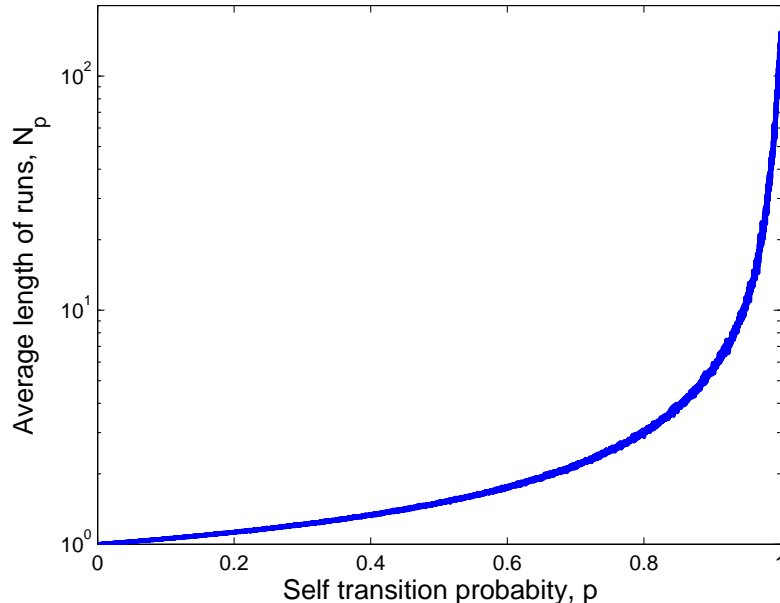


FIG. 5: Average length of runs N_p as a function of Markovian self-transition probability $p(=q)$ of spin +1 in the formation of magnetic domains. See text for details.

plot's width. Here data from anthropology, quantum theory and magnetic domain formation were invoked to exemplify the applicability of the approach.

Independent studies testing handedness in a mixture of cultures of chimpanzees were found to exhibit Markov memory assessed to a modest 64% probability of influence for the use of the right hand and no influential preference for the use of the left hand. A proportion of 58% of individuals showed preference for the use of their right hand. These quantified tendencies in handedness, influenced by human presence conveniently agree with independent anthropological studies.

The quantum Zeno effect as a Markovian memory process, exhibits either clustering or dispersion of the binary states both responsible for the hindering of state transitions. The self-transition probabilities responsible for the impedance of state transitions in the data by Balzer et al. were estimated. It is shown, for instance, that the Zeno effect is manifested through a combination of persistence of the initial Markovian binary state and a synchronous anti-persistence of the alternative state both at degrees which have been estimated.

Finally, the formation of simulated 2-D magnetic domains was discussed here as a third example of a process driven by Markovian memory. The self-transition probabilities for spin up or down were equal at the absence of a magnetic field. Depending on the strength of spin interactions a variety of domain formations arise, such as stripes, labyrinths or cells referred to at the order of their size. All three types were shown here to exhibit high self-transition probabilities above 80%.

APPENDIX A

Following the treatment of von Mises [20] we assume that $|p+q-1| \neq 1$ excluding the cases $p=q=1$ and $p=q=0$, as they present no interest but $0 < p, q < 1$. The following recursion formula holds for the state probabilities

$$p_i^{(n)} = \sum_{j=1}^2 p_{ij} p_j^{(n-1)}, \quad i = 1, 2; \quad n = 1, 2, \dots \quad (16)$$

Equations (16) are equivalent to the iteration set up of the following homogeneous equations

$$-x_i + \sum_{j=1}^2 p_{ij}x_j = 0, \quad i = 1, 2 \quad (17)$$

The sum of transition probabilities of each column is equal to 1. Also the absolute probabilities at every step of the system's evolution sum up to unity

$$\sum_{j=1}^2 p_{ij} = 1 \quad (18)$$

$$\sum_{j=1}^2 p_i^{(n)} = \sum_{j=1}^2 p_i^{(0)} = 1 \quad (19)$$

Since the 2x2 transition matrix having elements p_{ij} $i, j = 1, 2$ is regular, $\underline{p}^{(n)}$ tends to a unique fixed probability vector $\underline{p}^{(\infty)}$ that can be estimated by solving the system of Eqs. (17). These lead to two non-zero solutions u and $1 - u$, to which the probabilities p_n and $1 - p_n$ converge after a large number of trials, n . The two roots of system (17) are the values λ for which its determinant $|P(\lambda)|$ vanishes

$$|P(\lambda)| = \begin{vmatrix} p - \lambda & 1 - q \\ 1 - p & q - \lambda \end{vmatrix} = 0 \quad (20)$$

where λ cannot be greater than 1 in absolute value. In this case the two roots are

$$\begin{aligned} \lambda_1 &= p + q - 1 \\ \lambda_2 &= 1 \end{aligned} \quad (21)$$

The equations (16), and (21), can then be written as

$$\begin{aligned} u_1 &= p \cdot u_1 + (1 - q) \cdot u_2 \\ u_2 &= (1 - p) \cdot u_1 + q \cdot u_2 \end{aligned} \quad (22)$$

yielding the two not uniquely determined solutions u & $1 - u$

$$\begin{aligned} u \equiv \wp &= \lim_{n \rightarrow \infty} p_n = \frac{1 - q}{2 - (p + q)} \\ 1 - u \equiv 1 - \wp &= \frac{1 - p}{2 - (p + q)} \end{aligned} \quad (23)$$

Equations (23) have an important consequence. The probabilities of finding the system at either binary state after n trials converge to $\wp = 50\%$, provided the two self-transition probabilities are equal, $p = q$, and regardless if they are different from 50%. In other words, in the long run binary states (A and B) will occur in the Markov chain at the same frequency as if no memory was involved. From the point of view of long-run state probabilities the Markov process will resemble a memoryless Bernoulli case. We shall next estimate the frequency of state A.

As stated in the text, the number $x_\nu = 1$ is associated with the occurrence of state A after a measurement and $x_\nu = 0$ is associated with the occurrence of state B. The expectation value of x_ν , i.e. p_ν , will be the probability that

the outcome of the ν^{th} measurement will be the number 1. The expectation value of all the '1' states present in a Markov sequence of n trials will be then

$$E[x_1 + x_2 + \dots + x_n] = p_1 + p_2 + \dots + p_n \quad (24)$$

and the expected value of proportion of ones in the chain in will be

$$E\left[\frac{x}{n}\right] = \frac{p_1 + p_2 + \dots + p_n}{n} = \bar{p}_n \quad (25)$$

The recursion formula (16) can be written

$$p_n = \sum_{j=1}^2 p_{1j} p_j^{(n-1)} = p_{11} p_1^{(n-1)} + p_{12} p_2^{(n-1)} = a \cdot p_{n+1} + b \quad (26)$$

where $a = p + q - 1 \neq 1$, & $b = 1 - q$ since $0 < p < 1$ and $0 < q < 1$. Given that the initial value of p_n is $p_1^{(0)} = p_1$, the recursion formula (26) yields [33]

$$p_n = a^{(n-1)} p_1 + \underbrace{a^{n-2} + a^{n-3} + \dots + a + 1}_{(n-1) \text{ terms}} \cdot b = a^{n-1} p_1 + \frac{1 - a^{n-1}}{1 - a} \cdot b \quad (27)$$

or

$$p_n = a^{n-1} \left[p_1 - \frac{1 - q}{2 - (p + q)} \right] + \frac{1 - q}{2 - (p + q)} = a^{n-1} [p_1 - \wp] + \wp \quad (28)$$

where \wp is defined in (23). The average expected proportion of state A, p_n , in the chain of n trials would be written as [34]

$$\bar{p}_n = \frac{1}{n} \sum_{i=1}^n p_i = \frac{1}{n} (p_1 + p_2 + \dots + p_n) = \wp + \frac{p_1 - \wp}{n} \cdot \frac{1 - a^n}{1 - a} \quad (29)$$

and

$$\bar{p}_n \xrightarrow{n \rightarrow \infty} \wp \quad (30)$$

The absolute probability of finding the system at state A after n measurements of its state is written $p_1^{(n)} = p_n$ and the probability of finding it at state B is $p_2^{(n)} = 1 - p_n$. This is equivalent to saying that the n -th measurement of the system's state has a probability p_n of finding it at state A. Since $p^{(n)} = p_{11}^{(n)}$ & $q^{(n)} = p_{12}^{(n)}$ the recursion formula (16) applies to the transition probabilities between states too

$$p^{(n)} = a \cdot p^{(n-1)} + b$$

$$q^{(n)} = a \cdot q^{(n-1)} + b \quad (31)$$

The recursion formula then yields, since $p_{11}^{(0)} = 1$ & $p_{12}^{(0)} = 0$

$$p^{(n)} = a^n p^{(0)} + \underbrace{[a^{n-1} + a^{n-2} + \dots + a + 1]}_{n \text{ terms}} \cdot b = a^n + \frac{1 - a^n}{1 - a} \cdot b = a^n \cdot [1 - \wp] + \wp \quad (32)$$

and

$$q^{(n)} = a^n q^{(0)} + \underbrace{[a^{n-1} + a^{n-2} + \dots + a + 1]}_{n \text{ terms}} \cdot b = a^n \cdot [1 - \wp] \quad (33)$$

If the system is at state A the probability that after n steps, where n is very large, the measurement will yield again state A is \wp : $p^{(n)} \xrightarrow{n \rightarrow \infty} \wp$ and to yield state B is zero $q^{(n)} \xrightarrow{n \rightarrow \infty} 0$.

Von Mises has estimated the standard deviation of the mean value \wp , in other words, the asymptotic value of the standard deviation of the proportion of state A, \bar{p}_n , in the sequence of n trials as

$$\sigma = \sqrt{\frac{\wp(1-\wp)}{n}} \cdot \sqrt{\frac{1+a}{1-a}} = \sigma_o \cdot \nu \quad (34)$$

The proportion of state A in sequences of trials of length n of a Markov process with memory scatters about the asymptotic value \wp , while their scatter has been modulated with respect to the memory-less case

$$\sigma_o = \sqrt{\frac{\wp(1-\wp)}{n}} \quad (35)$$

The modulating variance factor in (34)

$$\nu = \sqrt{\frac{1+a}{1-a}} \quad (36)$$

takes values either above or below 1 depending on the self transition probabilities according to

$$\nu > 1 \Rightarrow p + q > 0.5$$

$$\nu < 1 \Rightarrow p + q < 0.5 \quad (37)$$

* Electronic address: Electronic Mail: fpallik@phys.uoa.gr

- [1] F. Galton, Natural Inheritance, MacMillan, London, 1889.
- [2] W.M. Itano, D.J. Heinzen, J.J. Bollinger and D.J. Wineland, Phys. Rev. A 41 (1990) 2295.
- [3] C. Balzer, R. Huesmann, W. Neuhauser and P.E. Toschek, Opt. Commun. 180 (2000) 115.
- [4] W.G. Hoover, B. Moran, C.G. Hoover and W.J. Evans, Phys. Lett. A 133 (1988) 114.
- [5] A.D. Chepelianskii and D.L. Shepelyansky, Phys. Rev. Lett. 87 (2001) 034101.
- [6] A. Lue and H. Brenner, Phys. Rev. E 47 (1993) 3128.
- [7] N. Papasimakis and F. Pallikari, in: Complexus Mundi: Emergent Patterns in Nature (ed. M.N. Novak), World Scientific Publishing Co., Singapore, 2006.
- [8] P. Martinot-Lagarde, H. Dreyfus-Lambeiz and I. Dozov, Phys. Rev. E 67 (2003) 051710.
- [9] Z.-L. Xie and H. Kwok, Jpn. J. Appl. Phys. 37 (1998) 2572.
- [10] S. Lamarque-Forget, O. Pelletier, I. Dozov, P. Davidson, P. Martinot-Lagarde and J. Livage, Adv. Mater. 70 (2000) 1267.
- [11] A. Barone, G. Kurizki and A.G. Kofman, Phys. Rev. Lett. 92 (2004) 200403.
- [12] J.K. Moser, IBM J. Res. Dev. 5 (1961) 226.
- [13] F. Ritort, J. Stat. Mech. Theory Exp. (2004) P10016.
- [14] A.J. de Craen, J. Gussekloo, B. Vrijisen and R.G. Westendorp, Am. J. Epidemiol. 161 (2005) 114.
- [15] A. Aleman, R. Hijman, E.H.F. de Haan and R.S. Kahn, Am. J. Psychiatry 156 (1999) 1358.
- [16] A.R. Palmer, Am. J. Phys. Anthropol. 118 (2002) 191.
- [17] P. Alderson, S. Green and J.P.T. Higgins (eds.), Cochrane Reviewers' Handbook 4.2.2, in: The Cochrane Library, Issue 1, John Wiley and Sons, Chichester, UK, 2004.
- [18] S. Waner and S. Costenoble, Finite Mathematics and Applied Calculus, Thomson-Brooks/Cole, 2004.
- [19] A.T. Bharucha-Reid, Elements of the Theory of Markov Processes and Their Applications, McGraw-Hill, New York, 1960.

- [20] R.V. Mises, *Mathematical Theory of Probability and Statistics*, Academic Press, New York, 1964.
- [21] Also termed the funnel plot due to its shape.
- [22] Trustworthiness of statistical results is, however, limited by insufficiently small databases and the presences of biases.
- [23] M. Schroeder, *Fractals, Chaos and Power Laws: minutes from an infinite paradise*, W. H. Freeman and Company, New York, 1991.
- [24] J.K. Breslin and G.J. Milburn, *Phys. Rev. A* 55 (1997) 1430.
- [25] A.M. Walker, J.M. Martin-Moreno and F.R. Artalejo, *Am. J. Public Health* 78 (1988) 961.
- [26] for lengths above $m \simeq 3$
- [27] Their reliability depends on the size of meta-analysis and the presence of biases.
- [28] A. Whiten, J. Goodall, W.C. McGrew, T. Nishida, V. Reynolds, Y. Sugiyama, C.E.G. Tutin, R.W. Wrangham and C. Boesch, *Nature* 399 (1999) 682.
- [29] in other words the runs of binary states
- [30] J.R. Iglesias, S. Goncalves, O.A. Nagel and M. Kiwi, *Phys. Rev. B* 65 (2002) 064447.
- [31] Data from figure 4 in reference [3].
- [32] Since the outcome of a measurement depends on previous measurements.
- [33] The sum of the converging geometric series ($a < 1$) has $n - 1$ terms.
- [34] The sum of the converging geometric series has now n terms.